

RESEARCH

Open Access



Heat-transfer performance of twisted tubes for highly viscous food waste slurry from biogas plants

Jingjing Chen^{1,2*}, Mikael Risberg¹, Lars Westerlund¹, Urban Jansson³, Changsong Wang², Xiaohua Lu² and Xiaoyan Ji^{1*}

Abstract

Background: The use of food waste as feedstock shows high production of biogas via anaerobic digestion, but requires efficient heat transfer in food waste slurry at heating and cooling processes. The lack of rheological properties hampered the research on the heat-transfer process for food waste slurry. Referentially, the twisted hexagonal and elliptical tubes have been proved as the optimal enhanced geometry for heat transfer of medium viscous slurries with non-Newtonian behavior and Newtonian fluids, respectively. It remains unknown whether improvements can be achieved by using twisted geometries in combination with food waste slurry in processes including heating and cooling.

Results: Food waste slurry was observed to exhibit highly viscous, significant temperature-dependence, and strongly shear-thinning rheological characteristics. Experiments confirmed the heat-transfer enhancement of twisted hexagonal tubes for food waste slurry and validated the computational fluid dynamics-based simulations with an average deviation of 14.2%. Twisted hexagonal tubes were observed to be more effective at low-temperature differences and possess an enhancement factor of up to 2.75; while twisted elliptical tubes only exhibited limited heat-transfer enhancement at high Reynolds numbers. The heat-transfer enhancement achieved by twisted hexagonal tubes was attributed to the low dynamic viscosity in the boundary layer induced by the strong and continuous shear effect near the walls of the tube.

Conclusions: This study determined the rheological properties of food waste slurry, confirmed the heat-transfer enhancement of the twisted hexagonal tubes experimentally and numerically, and revealed the mechanism of heat-transfer enhancement based on shear rate distributions.

Highlights

- Rheological properties of food waste slurry were tested and modeled
- Pilot test of twisted tube heat exchanger validated the CFD-based simulations
- Twisted hexagonal tubes exhibited better performance at low-temperature differences
- Heat-transfer enhancement was due to strong and continuous shear effect close to tube walls

*Correspondence: jingjingchen@njtech.edu.cn; xiaoyan.ji@ltu.se

¹ Energy Engineering, Division of Energy Science, Luleå University of Technology, 97187 Luleå, Sweden
Full list of author information is available at the end of the article



© The Author(s) 2022. **Open Access** This article is licensed under a Creative Commons Attribution 4.0 International License, which permits use, sharing, adaptation, distribution and reproduction in any medium or format, as long as you give appropriate credit to the original author(s) and the source, provide a link to the Creative Commons licence, and indicate if changes were made. The images or other third party material in this article are included in the article's Creative Commons licence, unless indicated otherwise in a credit line to the material. If material is not included in the article's Creative Commons licence and your intended use is not permitted by statutory regulation or exceeds the permitted use, you will need to obtain permission directly from the copyright holder. To view a copy of this licence, visit <http://creativecommons.org/licenses/by/4.0/>. The Creative Commons Public Domain Dedication waiver (<http://creativecommons.org/publicdomain/zero/1.0/>) applies to the data made available in this article, unless otherwise stated in a credit line to the data.

Twisted hexagonal tubes exhibited better performance at low-temperature differences

Heat-transfer enhancement was due to strong and continuous shear effect close to tube walls

Keywords: Food waste slurry, Rheological properties, Twisted tubes, Computational fluid dynamics, Heat-transfer enhancement

Background

Food waste, a type of typical organic solid waste, is produced in large quantities and can severely contaminate air, water, and soil if it is not collected, transported, and stored properly [1]. Fortunately, food waste is degradable and is used as a desirable substrate in the production of biogas via the anaerobic digestion (AD) process [2–4]. Mohsen et al. [5] designed a laboratory-scale semi-continuous membrane-assisted anaerobic reactor to produce biogas from food waste slurry (FWS) with a total solid (TS) content of 13%. They found that a considerable amount of biogas can be produced while consuming extremely low amounts of chemicals, such as alkalis and active carbon. Charles et al. [3] investigated FWS with TS = 10% in a pilot-scale 900 m³ AD reactor and reported a high production rate of 600 m³ of biogas (60% of methane) per ton of volatile solids (i.e., the flammable part of solids at 550 °C). In practice, food waste has emerged as a vital feedstock in the AD process in biogas plants in several European countries, including Ireland [6], Denmark [7], and Sweden [8].

Usually, the thermal energy used to maintain the temperature of AD reactors and preheat feed streams accounts for more than 70% of the total energy utilization in a biogas plant [9]. Especially when food waste is used as the substrate, sanitation at a high temperature (70 °C) is required to pasteurize the feeding slurries [10], leading to the consumption of additional thermal energy compared to processes based on other substrates. Moreover, following sanitation, a cooling process is required to decrease the temperature from 70 to 50 °C to fulfill the temperature requirements of AD reactors. This makes the use of highly efficient thermal systems essential to reduce thermal energy utilization. The heat exchanger is an important component in such systems. Although, currently, shell-and-tube heat exchangers with circular tubes are the most popular variant, developing novel heat exchangers to improve the efficiency of thermal systems is one of the most important topics of research in this field.

For developing novel heat exchangers, the properties of the working fluids, especially the rheological properties for non-Newtonian fluids, should be determined first. The main working fluids in the AD process are the slurries. Manure and corn straw slurries have been found to be the non-Newtonian fluids and show complex

properties for their shear-thinning, temperature-, and substrate-dependent rheological properties [11, 12]. Moreover, the rheological properties were found as the key to determining the flow and heat-transfer process for the slurries [13]. However, to the best of our knowledge, the rheological properties of food waste slurry are missing. This hindered the quantifications of experimental and numerical studies on the heat-transfer process for the food waste slurries.

The twisted tubes have been extensively approved as an effective passive technology for the heat-transfer enhancement of fluids with complex properties. In our previous studies, for the manure slurry (MS) [14] and corn straw slurry (CSS) [15], we screened twisted hexagonal tubes (THTs) from multiple twisted equilateral-polygon tubes using computational fluid dynamics (CFD)-based simulations, verified the enhanced performance of THTs with experiments, and integrated THTs into thermal systems of biogas plants. Our observations indicated that for the full-scale biogas plant, the implementation of optimally structured THTs in waste-heat recovery and the external heating processes significantly increase the net production of biofuel by up to 17% and conserve thermal energy by up to 39%, respectively. However, these studies focused on the heat-transfer performance including the heat-transfer coefficient, friction coefficient, and enhancement factor only compared to the circular tube in heating process (cool slurries and hot heat-exchange wall). The improvements achieved using THTs and commercialized twisted tubes in combination with other kinds of slurries, e.g., food waste, and in other processes, including heating and cooling, are yet to be established.

Twisted elliptical tubes (TETs) have been identified to be one of the most successful types of commercial heat exchangers in water treatment and chemical industries, and its enhancement factor (1.3–2.5) for simple fluids [16] is comparable to those of THTs for slurries. For slightly high viscous fluids, e.g., oil in the laminar region (0.030 Pa·s), significantly high enhancement factors up to 1.5 were obtained [17]; for engine oil (0.0033 Pa·s) and ethylene glycol (0.016 Pa·s), the enhancement factor was bounded by 0.94, and it was observed to decrease as the Reynolds number (*Re*) increased [18]. These results indicate that it might be worthwhile to extend the application of commercialized TET to slurries and compare its

performance with that of the THT. However, to the best of our knowledge, this topic has not yet been researched.

In this study, the heat-transfer performances of FWS in THT and TET were evaluated, using the circular tube (CT) as the reference. To this end, the rheological properties of FWS with TS=10% obtained from a biogas plant were tested and modeled. Based on these data, CFD-based simulations were conducted to predict the performance of heat exchangers with different geometries, and pilot-scale testing was performed to validate the numerical simulation results. Moreover, the performances of THT and TET in heating and cooling systems at different temperature differences were analyzed and compared to those of CT. Finally, the mechanism of heat-transfer enhancement was revealed.

Results and discussion

In this section, the determination and modeling of the rheological properties of FWS are described, and their implementation in the CFD-based simulation of the heat-transfer process is discussed. Subsequently, the experimental data on the heat-transfer performance of FWS in THT obtained via pilot-scale testing are described. Further, the validations of CFD simulations are determined, and heat-transfer coefficients, friction coefficients during heating and cooling phases in THT and TET are determined using CFD and compared to those of CT. Thereafter, the enhancement factors of THT and TET are calculated based on the numerical results. Moreover, the relationships between operating conditions, flow state, and heat-transfer performance of FWS in THT are established with respect to practical applications. Finally, the mechanism of heat-transfer enhancement is revealed.

Rheological properties of food waste slurry

Testing results

The rheological properties for FWS with TS=10% at temperatures between 10 °C and 70 °C and shear rates γ between 0.01 s⁻¹ and 100 s⁻¹ are listed in Additional file 1: Table S1 and depicted in Fig. 1. The dynamic viscosity of FWS is observed to be strongly dependent on temperature; it decreased by the factors of up to 2.2 at $\gamma=0.1$ s⁻¹ ($\mu=5658$ Pa·s at 10 °C vs. $\mu=2612$ Pa·s at 70 °C) and 3.5 at $\gamma=100$ s⁻¹ ($\mu=0.8814$ Pa·s at 10 °C vs. $\mu=0.2487$ Pa·s at 70 °C) when the temperature was increased from 10 to 70 °C. Shear rate is also observed to have a profound impact on the rheological properties of FWS. Low shear rates ($\gamma=0.1$ s⁻¹) induced ultra-high dynamic viscosities ($\mu=263$ –543 Pa·s) in FWS, which is similar to that of polymers, such as polyphenylene sulfide [19].

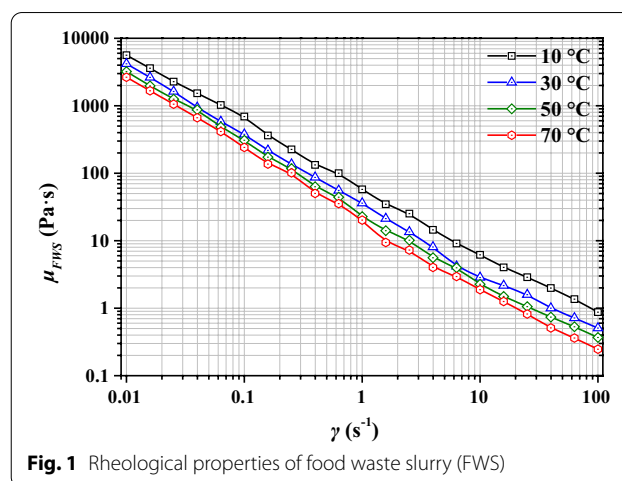


Fig. 1 Rheological properties of food waste slurry (FWS)

Table 1 Comparison of the dynamic viscosities of different slurries

| Slurries | T, °C | μ , Pa·s | |
|----------------------------|-------|------------------------------|------------------------------|
| | | $\gamma=100$ s ⁻¹ | $\gamma=0.1$ s ⁻¹ |
| FWS, TS = 10% (this study) | 10 | 0.72 | 543 |
| | 55 | 0.22 | 263 |
| MS, TS = 10% [20] | 10 | 0.32 | 38 |
| | 55 | 0.081 | 2.2 |
| CSS, TS = 8% [15] | 10 | 0.035 | 1.6 |
| | 55 | 0.032 | 0.75 |

Comparison of different slurries

A comparison of the rheological properties of different slurries is presented in Table 1. The viscosity of FWS was higher than those of MS and CSS by 1–2 orders of magnitude. However, at high shear rates ($\gamma=100$ s⁻¹), the dynamic viscosity of FWS was 2–3 times that of MS and one order of magnitude higher than that of CSS. The difference between the rheological properties of different slurries can be explained as follows. FWS and MS substrates comprise hydrophilic particles and soluble organics, while CSS is a typical lignocellulosic fiber suspension with hydrophobic behavior. In addition, FWS consists of larger organic molecules, e.g., starch, proteins, oils, and fats, compared to MS. Hence, the dynamic viscosity of FWS is higher than that of MS and much higher than that of CSS under identical shear conditions.

Modeling

According to previous studies [21], slurries obtained from biogas plants are typical shear-thinning and highly viscous fluids. The power law model, given by Eq. (1), has been used to describe non-Newtonian behavior reliably

in previous studies [12, 20]. Moreover, it is necessary to determine the critical-shear viscosity (CSV) and zero-shear viscosity (ZSV) of the rheology for application in the CFD-based simulations of the heat-transfer process of the slurries [22]. In this study, the tested rheological properties of FWS with TS=10% were modeled using Eq. (1). The characteristic parameters, including the consistency coefficient, k , the flow behavior index, n , the CSV, μ_{CSV} and the ZSV, μ_{ZSV} , were modeled using Eqs. (2), (3), (4), and (5), respectively. Considering the flattening tendency of γ in the range between 60 s^{-1} and 100 s^{-1} , as depicted in Fig. 1, μ_{CSV} was selected to be equal to μ at $\gamma=100 \text{ s}^{-1}$, and for the convergence of the simulation, μ_{ZSV} was selected to be equal to μ at $\gamma=0.01 \text{ s}^{-1}$:

$$\mu = k\gamma^{n-1}, \tag{1}$$

$$k = 0.101e^{\frac{1806.0}{T}}, R^2 = 0.968, \tag{2}$$

$$n = -0.00117T + 0.358, R^2 = 0.970, \tag{3}$$

$$\mu_{CSV} = 5.63 \times 10^{-4}e^{2072.8/T}, R^2 = 0.990, \tag{4}$$

$$\mu_{ZSV} = 74.4e^{1224.0/T}, R^2 = 0.973. \tag{5}$$

The characteristic parameters involved in the modeling of different slurries are listed in Table 2. For non-Newtonian fluids, a lower n represents stronger shear-thinning behavior. Thus, FWS slurry was observed to exhibit extremely strong shear-thinning behavior with the flow behavior, n being approximately equal to and less than zero at $10 \text{ }^\circ\text{C}$ and $55 \text{ }^\circ\text{C}$, respectively. In comparison, the values of n for CSS and MS are intermediate between 0.1 and 0.519. This indicates that the dynamic viscosity of FWS is much more sensitive to the shear effect compared to those of CSS and MS. k is a measure of the average viscosity of non-Newtonian fluids. The value of k for FWS is higher than those of CSS and MS by more than one order of magnitude. This explains the much higher viscosity of FWS compared to those of CSS and MS.

Results of the pilot test

A continuous test (5–10 h per day; 204 h in aggregate; between 1st and 30th April, 2021) was conducted to determine the K_i of FWS with TS=10% in THT heat exchangers at the Boden Biogas Plant, Sweden. The results of the pilot-scale experiment are illustrated in Fig. 2a. During the continuous test, obvious fluctuations were observed in the K_i values of the THTs. The flow rate of FWS was maintained at $5 \text{ m}^3/\text{h}$, while the temperature of the stream of FWS varied owing to the operations. Hence, the fluctuations of K_i were induced by the unstable temperature differences. The average value of K_i is $714 \text{ W}/(\text{m}^2\cdot\text{K})$, which is 2.20 times that of CT heat exchangers ($325 \text{ W}/(\text{m}^2\cdot\text{K})$) obtained in our previous tests [22]. The relationship between the K_i and the temperature difference, ΔT_m , was extracted from Fig. 2a and is illustrated in Fig. 2b. The results confirmed that K_i of

Table 2 Rheological parameters of different slurries

| Slurries | T, °C | k | n |
|----------------------------|-------|-------|---------|
| FWS, TS = 10% (this study) | 10 | 59.7 | 0.0409 |
| | 55 | 24.9 | -0.0239 |
| MS, TS = 10% [20] | 10 | 7.68 | 0.308 |
| | 55 | 0.739 | 0.519 |
| CSS, TS = 8% [15] | 10 | 1.57 | 0.178 |
| | 55 | 0.754 | 0.312 |

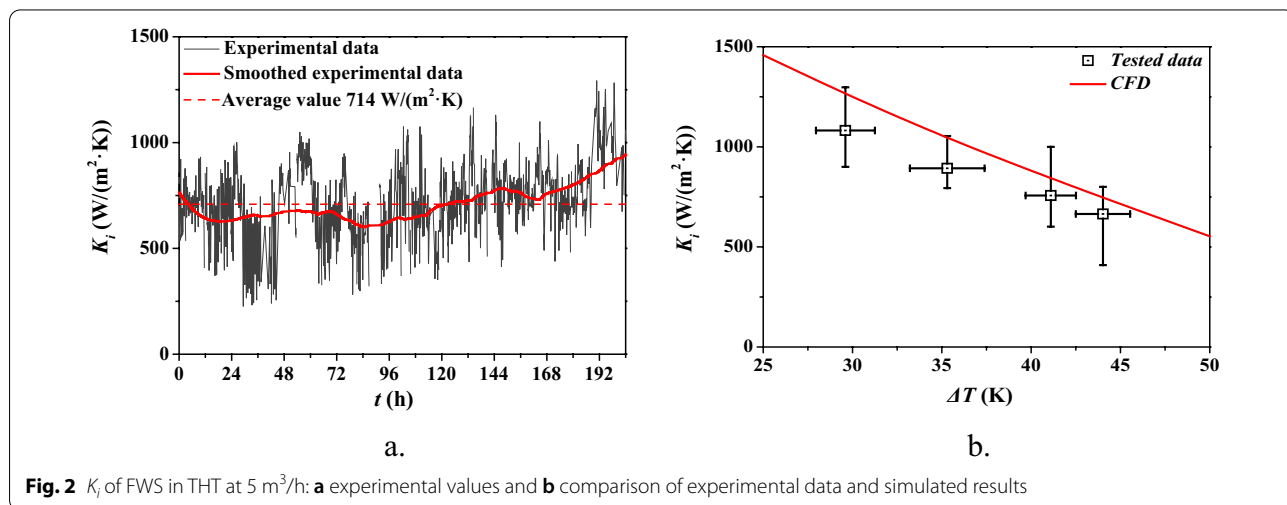


Fig. 2 K_i of FWS in THT at $5 \text{ m}^3/\text{h}$: **a** experimental values and **b** comparison of experimental data and simulated results

FWS in THT decreased with the increasing temperature difference.

Heat-transfer performance of food waste slurry in twisted tubes

Validation

Before systematically evaluating the heat-transfer performance of FWS in twisted tubes, the numerical results were validated by simulating the K_i values of FWS with $TS=10\%$ in THTs corresponding to temperature differences (ΔT , absolute value of T_w-T_s) ranging from 25 to 50 °C. The numerical CFD results, depicted in Fig. 5b, were validated by comparing them with the results obtained via pilot test. The average relative deviation (ARD) between the experimental and simulated results was 13.8%. Usually, ARDs between experimental and numerical results in the range of 10–15% represent reliable results in engineering [23]. Therefore, the CFD-based simulations are reliable.

Heat-transfer coefficients

Next, the heat-transfer coefficient K_i values of FWC in THT, TET, and TC during both heating and cooling processes [different wall and fluid-inlet temperatures (T_w and T_s)] were estimated numerically. The K_i values corresponding to different temperature differences are depicted in Fig. 3. FWS was observed to exhibit significantly higher $Nu/Pr^{1/3}$ in THT and TET than in CT at the same Re . Further, the K_i values of FWS in different tubes during heating and cooling phases were quite different.

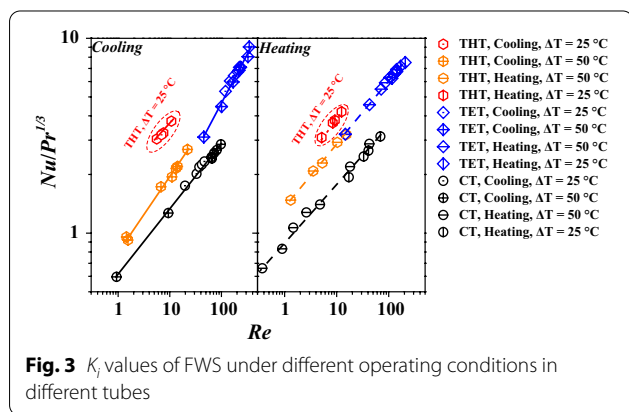


Fig. 3 K_i values of FWS under different operating conditions in different tubes

The numerical results of Nu were also correlated with Re and Pr , as recorded in Table 3. The correlation of the Nu of FWS in THT exhibited the same tendency as that in TET corresponding to large $\Delta T=50$ °C [see Eqs. (3) and (5); (4) and (6) in Table 5]. Significantly, FWC exhibited better heat transfer in THT compared to TET at $\Delta T=25$ °C. K_i of FWC in TET and CT was observed to be hardly dependent on ΔT . This indicates that THT possesses an advantage in terms of heat exchange during various thermal processes, including heating, cooling, sanitation, and waste-heat recovery, in FWS-based biogas plants, over TET and CT at low-temperature differences.

Friction coefficients

The friction coefficient f should be considered during the application of an enhanced geometry to a heat-transfer process. Thus, the values of f for THT, TET, and CT corresponding to different values of Re and Pr were determined using CFD-based simulations. The results are illustrated in Fig. 4. The values of f of THT and CT exhibited similar trends ($f \cdot Pr^{1/3} = 116Re^{-0.711}$), while that of TET followed the equation, $f \cdot Pr^{1/3} = 577Re^{-0.876}$. This indicates that the flow resistance in THT is similar to that in CT and much lower than that in TET. For Newtonian fluids, the friction can be reportedly increased by up to 1.9 times in TET compared to that in CT ($f_{TET}/f_{CT}=1.9$) [24] in the laminar region, and a decrease in the relative

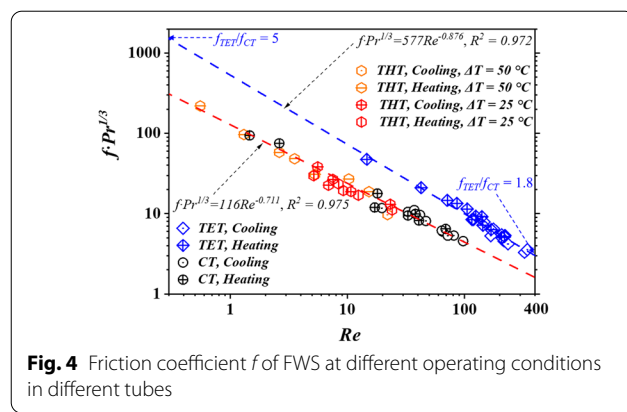


Fig. 4 Friction coefficient f of FWS at different operating conditions in different tubes

Table 3 Correlations of Re , Pr , and Nu in different tubes

| Tubes | Equations | |
|-----------------------|---|---|
| | Cooling | Heating |
| THT, $\Delta T=25$ °C | 1. $Nu = 1.69Re^{0.335}Pr^{1/3}$, $R^2 = 0.973$ | 2. $Nu = 1.76Re^{0.346}Pr^{1/3}$, $R^2 = 0.999$ |
| THT, $\Delta T=50$ °C | 3. $Nu = 0.798Re^{0.387}Pr^{1/3}$, $R^2 = 0.993$ | 4. $Nu = 1.54Re^{0.265}Pr^{1/3}$, $R^2 = 0.943$ |
| TET | 5. $Nu = 0.422Re^{0.523}Pr^{1/3}$, $R^2 = 0.984$ | 6. $Nu = 1.36Re^{0.325}Pr^{1/3}$, $R^2 = 0.996$ |
| CT | 7. $Nu = 0.617Re^{0.337}Pr^{1/3}$, $R^2 = 0.995$ | 8. $Nu = 0.902Re^{0.295}Pr^{1/3}$, $R^2 = 0.993$ |

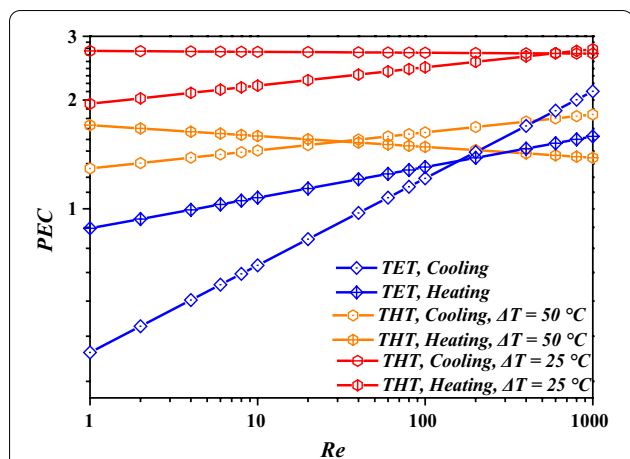


Fig. 5 Enhancement factors of different twisted tubes corresponding to different temperature differences

value, f_{TET}/f_{CT} , is observed at Reynolds numbers ranging between 250 and 400 [25]. In the present study, for the highly viscous FWS, f_{TET}/f_{CT} was observed to be 5–1.8 corresponding to Re lying in 0.3–400, indicating its advantage over TET in terms of the flow resistance, especially corresponding to low values of Re .

Enhancement factors

In principle, the comprehensive enhancement factor—the performance evaluation criteria (PEC)—should be considered while designing enhanced geometries; the value of PEC is directly proportional to the quality of the heat-transfer performance, and $PEC > 1.5$ has been recommended for engineering applications [26]. The values of PEC of THT, TET, and CT were calculated based on the obtained Nu and f . The results are illustrated in Fig. 5. A considerable heat-transfer enhancement (with PEC up to 2.75) was achieved for FWS in THT with $\Delta T = 25$ °C, while PEC was in the range of 1.2–1.8 for $\Delta T = 50$ °C. Usually, ΔT decreases as the heat-transfer process progresses. For example, when the temperature of the working fluid is gradually increased by increasing the temperature of the walls of the tube, the transferred heat from the wall to the working fluid gradually decreases because the heat-transfer coefficient Nu changes slightly for normal heat exchangers (refer TET and CT in Fig. 3). Hence, THT is promising for practical applications of FWS in biogas plants for its increased K_i at low-temperature differences. Moreover, TET performs worse than even CT at $Re < 5$ and 50 for heating and cooling processes, respectively, while it exhibits relatively weak advantages over CT at $Re > 400$ compared to THT. Therefore, TET heat exchangers are not recommended for application in biogas plants handling FWS.

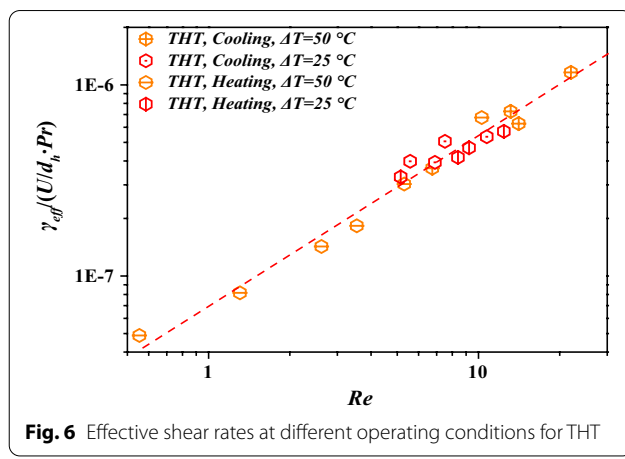


Fig. 6 Effective shear rates at different operating conditions for THT

Engineering equation

The effective shear rate γ_{eff} has been used to quantify the effective dynamic viscosity, μ_{eff} [14, 27]. The relationship between γ_{eff} and the operating conditions is displayed in Fig. 6 and regressed using Eq. (6). Using this relationship, K_i and PEC of FWS in THT can be determined directly from the tested properties and operating conditions. For engineering applications, γ_{eff} can be determined with Eq. (6). Subsequently, μ_{eff} can be calculated with Eqs. (1)–(3). Finally, the heat-transfer coefficient K_i can be calculated with Eqs. (7) and (8), the correlated Eqs. 1–4 in Table 3, and Eq. (9):

$$\gamma_{eff} = 7.09 \times 10^{-8} \frac{U}{d_h} Re^{0.881} Pr, R^2 = 0.920, \tag{6}$$

$$Re = \frac{d_h U \rho}{\mu_{eff}}, \tag{7}$$

$$Pr = \frac{\mu_{eff} C_p}{\lambda}, \tag{8}$$

$$Nu = \frac{K_i d_h}{\lambda}. \tag{9}$$

Mechanism of heat-transfer enhancement

For highly viscous FWS, THT exhibits a considerably high value of K_i with relatively low friction compared to TET, leading to superior enhancement compared to CT. Moreover, THT exhibits better heat transfer at lower temperature differences. To reveal the mechanism of these enhancements, it is essential to understand the dynamic viscosity and shearing state in tubes for FWS with non-Newtonian behavior.

In this part, firstly, the ratio of the dynamic viscosity in the boundary layer and bulk (μ_{bl}/μ_{eff}) and shear rate distributions in different tubes were sampled from the numerical results and analyzed. In our previous study [15], the average value of the shear rate γ_{avg} inside twisted can be used to represent the shear effect near the walls of the tubes. Hence, the dynamic viscosity in the boundary layer μ_{bl} was calculated based on γ_{avg} (refer to Additional file 1: Tables S2, S3, and S4 in supplementary material) obtained using CFD-based simulation following Eq. (4) and μ_{eff} was determined with Eq. (6). Subsequently, because the shearing state inside tubes determine the viscosity in tubes, the distributions of shear rate at different conditions were further analyzed.

Viscosities in boundary layer

The values of μ_{bl}/μ_{eff} in different tubes are illustrated in Fig. 7. THT and CT exhibited similar trends in dynamic viscosity with respect to Re , while TET exhibited a much higher dynamic viscosity in the boundary layer. This explains the lower flow resistance in THT compared to that in TET. However, the trend of μ_{bl}/μ_{eff} of THT indicates increased mixing, as represented by Re , and lower contribution to the reduction of the dynamic viscosity in the boundary layer compared to bulk flow. In TET, μ_{bl}/μ_{eff} was observed to decrease with an increase in Re . Such dependence trends of μ_{bl}/μ_{eff} on Re explain the heat-transfer enhancements achieved using THT and TET at low and high values of Re , respectively, as depicted in Fig. 5.

Shear rate distributions

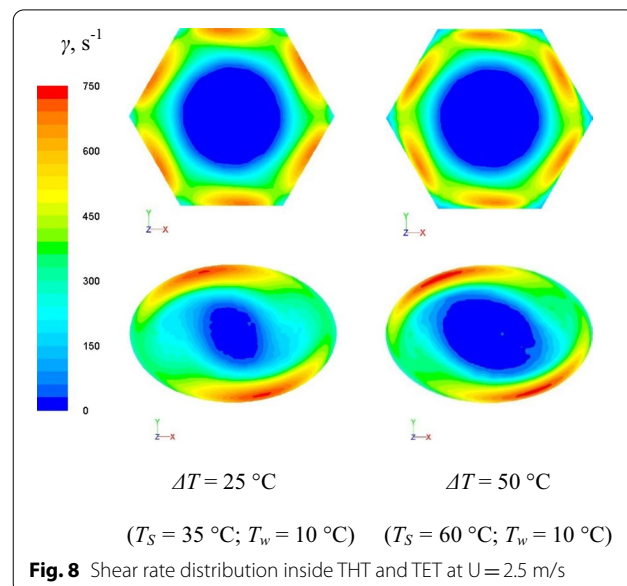
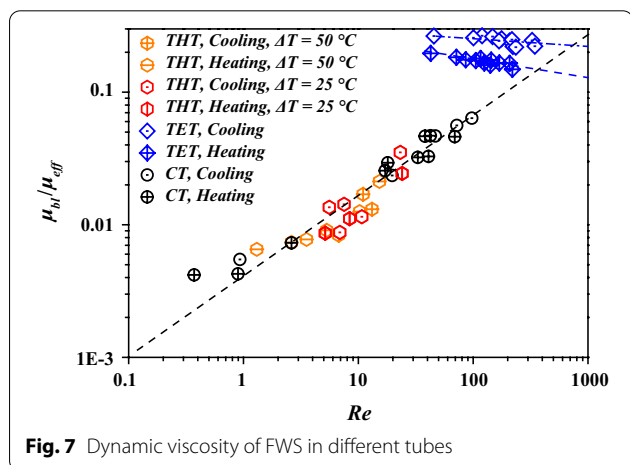
Higher heat-transfer performance of FWS in THT was observed at lower temperature difference in experiments, as shown in Fig. 2b. However, the dynamic viscosities in the boundary layer in THT corresponding to varying values of ΔT were observed to exhibit the same tendency

as that depicted in Fig. 7. A comparison of the shear rate distributions in THT and TET is depicted in Fig. 8. As established in our previous study [15], the strong and continuous shear effect near the walls of the tube leads to the strong and continuous local K_i . The region near the walls in THT where the shear force was strong ($\gamma > 600 \text{ s}^{-1}$) was observed to be larger than its counterpart in TET. This explains the superior performance of THT compared to TET. Moreover, as shown in Fig. 8, although FWS exhibited a similar shear rate distribution at $\Delta T = 25$ and $50 \text{ }^\circ\text{C}$ in THT, leading to the same tendency of μ_{bl}/μ_{eff} it is apparent that the strong and continuous shear effect in the case of $\Delta T = 25 \text{ }^\circ\text{C}$ is constrained to a region that is closer to the walls than in the case of $\Delta T = 50 \text{ }^\circ\text{C}$, leading to the lower-viscosity region close to the heat-exchange wall. This explains the higher degree of heat-transfer enhancement achieved using THT corresponding to low values of ΔT .

Conclusions

This study determined the rheological properties of food waste slurry, confirmed the heat-transfer enhancement of the twisted hexagonal tubes experimentally and numerically, and revealed the mechanism of heat-transfer enhancement based on shear rate distributions.

FWS was observed to exhibit a strong temperature-dependence and an extremely high shear-thinning dynamic viscosity. The numerical method used in this study was verified to be reliable. Enhancement factors of up to 2.75 were achieved in THT at low-temperature differences. In contrast, TET exhibited a weakened performance compared to even CT at a low Re and limited enhancement at a high Re . Moreover, the cause of the



heat-transfer enhancement in THT was identified as the strong and continuous shear rate close to wall.

The methodologies proposed in this study are expected to be useful as a reference for future studies on heat-transfer characteristics of non-Newtonian fluids with high dynamic viscosities.

Materials and methods

In this section, the methodology used to test and model the rheology of FWS are described. Details of the numerical models used to determine the heat-transfer performance of THT, TET, and CT as well as those of the pilot-scale testing in a biogas plant are presented.

Rheological properties of food waste slurry

FWS with TS=10% was sampled from Boden Biogas Plant, Sweden, as depicted in Fig. 9. Its rheological properties were measured using a rheometer (ARES G2, TA Instruments, New Castle, DE, USA) equipped with a helical ribbon impeller in a 34 mm diameter cup located at the Research Institutes of Sweden. The samples were pre-sheared at a shear rate of 50 s^{-1} for 10 s to compensate for any possible sedimentation. Pre-tests were repeated three times using fresh samples at $10 \text{ }^\circ\text{C}$, and an average deviation of 11.8% was observed. During testing, shearing was initiated using a low shear rate, and it was increased slowly to avoid sedimentation ($\dot{\gamma}=100-0.01 \text{ s}^{-1}$) at a specific temperature. Rheological properties were tested over a range of temperatures—at 10, 20, 30, 40, 50, 60,

and $70 \text{ }^\circ\text{C}$. The tested rheology was modeled and used as input for the CFD-based model.

Numerical modeling of food waste slurry in twisted tubes

In our previous studies [14, 15, 22], the optimal numerical schemes and meshes for CTs and twisted tubes corresponding to slurries obtained from biogas plants were addressed and experimentally validated. Hence, the geometries and boundary conditions adopted in this study are discussed briefly. In addition, the method used for the data reduction of numerical results is also provided below.

Geometries and computational domains

Figure 10 depicts the geometrical characteristics of THT and TET. The meshes are also illustrated, with cross-sections centered on the centerline. The geometrical parameters of THT, TET, and CT are listed in Table 4. The cross-section at the position, $z=0.8 \text{ m}$, in the axial direction was selected to display the details of shear rate distributions in twisted tubes, where the flow is fully developed, stable, and ready for analysis.

Boundary conditions

The flow of the slurry within the twisted tubes and the associated heat-transfer processes were simulated assuming the thermostatic wall condition under constant wall temperature (T_w). The specific boundary values of the inlet velocity (U) and inlet temperature (T_s) are summarized in Table 5. Combinations of these boundary



Fig. 9 FWS with TS = 10% obtained from Boden Biogas Plant, Sweden

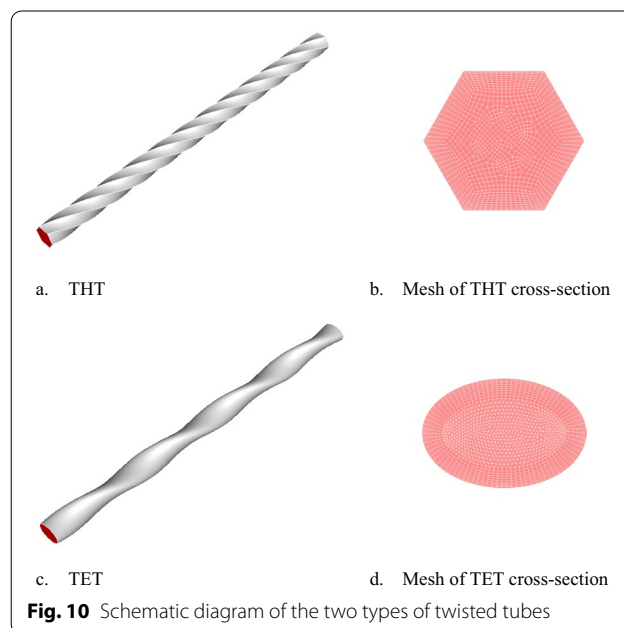


Fig. 10 Schematic diagram of the two types of twisted tubes

Table 4 Details of the geometries

| | Feature size, m | d_h , m | L , m | S , m | δ , mm |
|-----|---------------------------|-----------|---------|---------|---------------|
| THT | $l=0.030$ m | 0.0520 | 1 | 0.5 | 1 |
| TET | $a=0.0326$ m $b=0.0224$ m | 0.0506 | 1 | 0.5 | 1 |
| CT | – | 0.0573 | 1 | – | 1 |

conditions used in specific simulation cases are listed in Additional file 1: Tables S2, S3, and S4 in the additional material. The no-slip boundary condition was assumed in all simulation cases.

Data reduction of numerical results

In the convergent cases, the effective dynamic viscosity (μ_{eff}), inner wall temperature ($T_{w,i}$), volumetric average of the temperature of FWS ($T_{s,avg}$), wall-heat flux (q), and pressure drop (ΔP), were obtained directly from the CFD-based simulations. The heat-transfer coefficient K_i was calculated with Eq. (10). The friction coefficient (f) was determined using Eq. (11). Subsequently, the comprehensive parameter, i.e., PEC was calculated using Eq. (12) as the enhancement factor for twisted tubes:

$$K_i = \frac{q}{T_{w,i} - T_{s,avg}}, \quad (10)$$

$$f = \frac{2d_h \Delta P}{\rho U^2}, \quad (11)$$

$$PEC = \frac{Nu}{Nu_{CT}} \left(\frac{f}{f_{CT}} \right)^{1/3}, \quad (12)$$

where heat flux q , temperature of inner wall $T_{w,i}$, and average temperature of slurry in tubes $T_{s,avg}$ are obtained from CFD simulations; the properties of slurry density ρ , heat capacity c_p , and thermal conductivity λ were calculated according to previous study.

Table 5 Boundary conditions applied in CFD-based simulation

| State | T_s , °C | T_w , °C | U , m/s |
|---------|------------|------------|-----------|
| Heating | 10 | 60 | 1.0, 1.5 |
| | 35 | 60 | 2.0, 2.25 |
| | 60 | 10 | 2.5, 2.75 |
| Cooling | 60 | 10 | 3.0 |
| | 35 | 10 | |

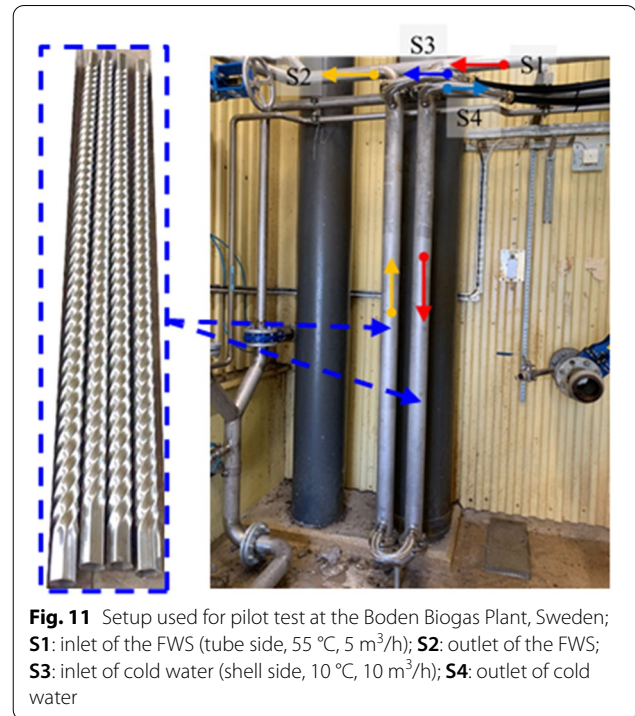


Fig. 11 Setup used for pilot test at the Boden Biogas Plant, Sweden; **S1**: inlet of the FWS (tube side, 55 °C, 5 m³/h); **S2**: outlet of the FWS; **S3**: inlet of cold water (shell side, 10 °C, 10 m³/h); **S4**: outlet of cold water

Pilot-scale testing

THTs were manufactured and installed as a type of shell-and-tube heat exchanger at the Boden Biogas Plant, Sweden. Their geometric parameters were taken to be identical to those of the “model”, as listed in Table 4. The diameter of the shell side was 0.08 m and the total length of the heat exchangers was 4.4 m. As depicted in Fig. 11, the working fluid was taken to be FWS with TS=10%. The inlet volume flow rate and temperature of the FWS on the tube side were maintained at 10 m³/h and 55 °C, respectively. The inlet volume flow rate and temperature of the cooling water on the shell side were maintained at 10 m³/h and 10 °C, respectively. The outlet temperatures on both the tube and shell sides were recorded using Pt-100 temperature sensors. The heat-transfer coefficient (K_i), of THT was calculated using the method described in our previous study [15].

Abbreviations

AD: Anaerobic digestion; FWS: Food waste slurry; TS: Total solid; THT: Twisted hexagonal tube; CFD: Computational fluid dynamics; MS: Manure slurry; CSS: Corn straw slurry; TET: Twisted elliptical tube; CT: Circular tube; CSV: Critical-shear viscosity; ZSV: Zero-shear viscosity; ARD: Average relative deviation; PEC: Performance evaluation criteria.

List of symbols

Re: Reynolds number; *Nu*: Nusselt number; *Pr*: Prandtl number; *k*: Consistency coefficient; *n*: Flow behavior index; *K_f*: Heat-transfer coefficient, W/(m²·K); *T*: Temperature, °C; ΔT : Temperature difference of wall and fluid, °C; ΔP : Pressure drop, Pa; *f*: Friction coefficient; *U*: Velocity, m/s; *d_h*: Hydraulic diameter, m; *L*: Length of the tubes, m; *S*: Torque of tubes, m; *c_p*: Heat capacity, J/(kg·K); *q*: Heat flux, W/m².

Greek alphabets

γ : Shear rate, s⁻¹; μ : Dynamic viscosity, Pa·s; δ : Thickness of tubes, m; ρ : Density, kg/m³; λ : Thermal conductivity of slurry, W/(m·K).

Subscripts

s: Slurry; *w*: Wall; *eff*: Effective; *avg*: Average; *bl*: Boundary layer; *i*: Inner.

Supplementary Information

The online version contains supplementary material available at <https://doi.org/10.1186/s13068-022-02156-4>.

Additional file 1: Table S1. Tested data of rheological properties for FWS with TS = 10%. **Table S2.** Numerical results of FWS in THT. **Table S3.** Numerical results of FWS in TET. **Table S4.** Numerical results of FWS in CT

Acknowledgements

Not applicable.

Author contributions

JC tested and modeled the rheological properties, validated the numerical models, conducted the CFD simulations, evaluated the results, and wrote the manuscript. MR and LW provided the numerical methods for CFD simulations. UJ installed the twisted-hexagonal-tube heat exchanger in Boden Biogas Plant and provided the samples of the food waste slurry. CW and XL participated in the planning. XJ edited the paper and contributed with results and discussion. All authors read and approved the final manuscript.

Funding

Open access funding provided by Lulea University of Technology. This work was supported by the Swedish Energy Agency (Grant No. 45957-1) and the National Natural Science Foundation of China (Grant Nos. 21838004 and 91934302).

Availability of data and materials

The data supporting the conclusions of this article are included with the article and its supplementary material.

Declarations**Ethics approval and consent to participate**

Not applicable.

Consent for publication

Not applicable.

Competing interests

The authors declare that they have no competing interests.

Author details

¹Energy Engineering, Division of Energy Science, Luleå University of Technology, 97187 Luleå, Sweden. ²State Key Laboratory of Material-Oriented Chemical Engineering, Nanjing Tech University, 210009 Nanjing, People's Republic of China. ³Boden Biogas Plant, Smidesvägen 3, 96138 Boden, Sweden.

Received: 22 March 2022 Accepted: 11 May 2022

Published online: 06 July 2022

References

- Braguglia CM, Gallipoli A, Gianico A, Pagliaccia P. Anaerobic bioconversion of food waste into energy: a critical review. *Biores Technol.* 2018;248:37–56.
- Browne JD, Murphy JD. Assessment of the resource associated with biomethane from food waste. *Appl Energy.* 2013;104:170–7.
- Banks CJ, Chesshire M, Heaven S, Arnold R. Anaerobic digestion of source-segregated domestic food waste: performance assessment by mass and energy balance. *Biores Technol.* 2011;102:612–20.
- Hedlund FH, Madsen M. Incomplete understanding of biogas chemical hazards—Serious gas poisoning accident while unloading food waste at biogas plant. *J Chem Health Saf.* 2018;25:13–21.
- Parchami M, Wainaina S, Mahboubi A, l'Ons D, Taherzadeh MJ. MBR-assisted VFAs production from excess sewage sludge and food waste slurry for sustainable wastewater treatment. *Appl Sci.* 2020;10:2921.
- Long A, Murphy JD. Can green gas certificates allow for the accurate quantification of the energy supply and sustainability of biomethane from a range of sources for renewable heat and or transport? *Renew Sustain Energy Rev.* 2019;115: 109347.
- Bundgaard SS, Kofoed-Wiuff A, Herrmann IT, Karlsson KB. Experiences with biogas in Denmark. DTU management engineering. 2014.
- Association SG. Proposal for national biogas strategy 2.0. Swedish gas association: Energigas Sverige, Stockholm. 2018.
- Lettinga G, Rebac S, Zeeman G. Challenge of psychrophilic anaerobic wastewater treatment. *Trends Biotechnol.* 2001;19:363–70.
- Thorin E, Lindmark J, Nordlander E, Odlare M, Dahlquist E, Kastensson J, et al. Performance optimization of the Växtkraft biogas production plant. *Appl Energy.* 2012;97:503–8.
- Achkari-Begdouri A, Goodrich PR. Rheological properties of Moroccan dairy cattle manure. *Biores Technol.* 1992;40:149–56.
- Tian L, Shen F, Yuan H, Zou D, Liu Y, Zhu B, et al. Reducing agitation energy-consumption by improving rheological properties of corn stover substrate in anaerobic digestion. *Biores Technol.* 2014;168:86–91.
- Wu B. Integration of mixing, heat transfer, and biochemical reaction kinetics in anaerobic methane fermentation. *Biotechnol Bioeng.* 2012;109:2864–74.
- Chen J, Risberg M, Westerlund L, Jansson U, Lu X, Wang C, et al. A high efficient heat exchanger with twisted geometries for biogas process with manure slurry. *Appl Energy.* 2020;279:115871.
- Chen J, Hai Z, Lu X, Wang C, Ji X. Heat-transfer enhancement for corn straw slurry from biogas plants by twisted hexagonal tubes. *Appl Energy.* 2020;262: 114554.
- Asmantas L, Nemira M, Trilikauskas V. Coefficients of heat transfer and hydraulic drag of a twisted oval tube. *Heat Transfer Soviet Research.* 1985;17:103–9.
- Sajadi A, Sorkhabi SYD, Ashtiani D, Kowsari F. Experimental and numerical study on heat transfer and flow resistance of oil flow in alternating elliptical axis tubes. *Int J Heat Mass Transf.* 2014;77:124–30.
- Khoshvaght-Aliabadi M, Arani-Lahtari Z. Forced convection in twisted minichannel (TMC) with different cross section shapes: a numerical study. *Appl Therm Eng.* 2016;93:101–12.
- Mihai M, Stoeffler K, Norton E. Use of thermal black as eco-filler in thermoplastic composites and hybrids for injection molding and 3D printing applications. *Molecules.* 2020;25:1517.
- Achkari-Begdouri A, Goodrich PR. Rheological properties of Moroccan dairy cattle manure ★. *Biores Technol.* 1992;40:149–56.
- Liu Y, Chen J, Song J, Hai Z, Lu X, Ji X, et al. Adjusting the rheological properties of corn-straw slurry to reduce the agitation power consumption in anaerobic digestion. *Biores Technol.* 2019;272:360–9.
- Chen J, Wu J, Ji X, Lu X, Wang C. Mechanism of waste-heat recovery from slurry by scraped-surface heat exchanger. *Appl Energy.* 2017;207:146.
- Zhang Z, Zhang W, Zhai ZJ, Chen QYH, Research R. Evaluation of Various Turbulence Models in Predicting Airflow and Turbulence in Enclosed Environments by CFD: Part 2—Comparison with Experimental Data from Literature. 2007;13:871–86.
- Guo A-N, Wang L-B. Parametrization of secondary flow intensity for laminar forced convection in twisted elliptical tube and derivation of loss coefficient and Nusselt number correlations by numerical analysis. *Int J Therm Sci.* 2020;155: 106425.

25. Cheng J, Qian Z, Wang Q. Analysis of heat transfer and flow resistance of twisted oval tube in low Reynolds number flow. *Int J Heat Mass Transf.* 2017;109:761–77.
26. Bhadouriya R, Agrawal A, Prabhu S. Experimental and numerical study of fluid flow and heat transfer in a twisted square duct. *Int J Heat Mass Transf.* 2015;82:143–58.
27. Metzner AB, Reed JC. Flow of non-newtonian fluids—correlation of the laminar, transition, and turbulent-flow regions. *AIChE J.* 1955;1(4):434–40.

Publisher's Note

Springer Nature remains neutral with regard to jurisdictional claims in published maps and institutional affiliations.

Ready to submit your research? Choose BMC and benefit from:

- fast, convenient online submission
- thorough peer review by experienced researchers in your field
- rapid publication on acceptance
- support for research data, including large and complex data types
- gold Open Access which fosters wider collaboration and increased citations
- maximum visibility for your research: over 100M website views per year

At BMC, research is always in progress.

Learn more biomedcentral.com/submissions

